The HSP90 inhibitor onalespib potentiates ^{177}Lu-DOTATATE therapy in neuroendocrine tumor cells

SARA LUNDSTEN[1], DIANA SPIEGELBERG[1,2], BO STENERLÖW[1] and MARIKA NESTOR[1]

Departments of [1]Immunology, Genetics and Pathology, and [2]Surgical Sciences, Uppsala University, 751 87 Uppsala, Sweden

Received March 8, 2019; Accepted July 19, 2019

DOI: 10.3892/ijo.2019.4888

Abstract. ^{177}Lu-DOTATATE was recently approved for the treatment of somatostatin receptor (SSTR)-positive neuroendocrine tumors (NETs). However, despite impressive response rates, complete responses are rare. Heat shock protein 90 (HSP90) inhibitors have been suggested as suitable therapeutic agents for NETs, as well as a potential radiosensitizers. Consequently, the aim of this study was to investigate whether the HSP90-inhibitor onalespib could reduce NET cell growth and act as a radiosensitizer when used in combination with ^{177}Lu-DOTATATE. The NET cell lines BON, NCI-H727 and NCI-H460, were first characterized with regards to ^{177}Lu-DOTATATE uptake and sensitivity to onalespib treatment in monolayer cell assays. The growth inhibitory effects of the monotherapies and combination treatments were then examined in three-dimensional multicellular tumor spheroids. Lastly, the molecular effects of the treatments were assessed. ^{177}Lu-DOTATATE uptake was observed in the BON and NCI-H727 cells, while the NCI-H460 cells exhibited no detectable uptake. Accordingly, ^{177}Lu-DOTATATE reduced the growth of BON and NCI-H727 spheroids, while no effect was observed in the NCI-H460 spheroids. Onalespib reduced cell viability and spheroid growth in all three cell lines. Furthermore, the combination of onalespib and ^{177}Lu-DOTATATE exerted synergistic therapeutic effects on the BON and NCI-H727 spheroids. Western blot analysis of BON spheroids revealed the downregulation of epidermal growth factor receptor (EGFR) and the upregulation of γ H2A histone family member X (γH2AX) following combined treatment with onalespib and ^{177}Lu-DOTATATE. Moreover, flow cytometric analyses revealed a two-fold increase in caspase 3/7 activity in the combination group. In conclusion, the findings of this study demonstrate that onalespib exerts antitumorigenic effects on NET cells and may thus be a feasible treatment option for NETs. Furthermore, onalespib was able to synergistically potentiate ^{177}Lu-DOTATATE treatment in a SSTR-specific manner. The radiosensitizing mechanisms of onalespib involved the downregulation of EGFR expression and the induction of apoptosis. Consequently, the combination of onalespib and ^{177}Lu-DOTATATE may prove to be a promising strategy with which to improve therapeutic responses in patients with NETs. Further studies investigating this strategy *in vivo* regarding the therapeutic effects and potential toxicities are warranted to expand these promising findings.

Introduction

Peptide receptor radionuclide therapy (PRRT) with radiolabeled somatostatin analogs has for >25 years been used for the delivery of therapeutic radionuclides to somatostatin receptor (SSTR)-positive neuroendocrine tumors (NETs) (1). As a result of the comprehensive NETTER-1 study, PRRT with the somatostatin analog, ^{177}Lu-DOTATATE (Lutathera), was recently approved for the treatment of gastroenteropancreatic NETs (2). The study concluded that PRRT significantly increased disease-free survival and prolonged overall survival compared to standard care; however, complete response was rare (2).

Therefore, ongoing research focuses on improving PRRT with ^{177}Lu-DOTATATE, for example by enhancing the affinity of peptides, the use of intra-arterial injection, or various combinations of peptides and radionuclides (3-5). In this respect, the possibility to use alpha emitters, such as ^{213}Bi and ^{225}Ac is currently being explored (6-8). Another strategy with which to enhance the treatment efficacy is the use of radiosensitizers, e.g. drugs that can potentiate the effects of radiation (9). One promising approach is the inhibition of molecular chaperones of the heat shock protein (HSP) family, such as HSP90, that regulate and stabilize a large number of oncogenic client proteins (10), of which several are involved in DNA damage response (DDR) (11).

Apart from its promising effects on radiosensitization, HSP90 inhibition has also been suggested as a suitable antitumorigenic strategy in NETs. Histopathological analyses have revealed a high expression of HSP90 in primary tumors and metastases (12,13), and the inhibition of HSP90 has been demonstrated to exert anti-proliferative effects on NET cells (12-15). HSP90 is upstream of e.g., both mammalian target of rapamycin (mTOR) and mitogen-activated protein

Correspondence to: Dr Marika Nestor, Department of Immunology, Genetics and Pathology, Uppsala University, The Rudbeck Laboratory, 751 87 Uppsala, Sweden
E-mail: marika.nestor@igp.uu.se

Key words: neuroendocrine neoplasms, neuroendocrine tumors, peptide receptor radionuclide therapy, ^{177}Lu-DOTATATE, Lutathera, heat shock protein 90, onalespib, AT13387, radiosensitization

kinase (MAPK)/extracellular-signal-regulated kinase (ERK) pathways, controlling the expression of growth factor receptors, such as epidermal growth factor (EGFR) and insulin-like growth factor 1 receptor (IGF1R), which initiate signaling (16). Mechanistic analyses using NET cell lines have concluded that the extensive crosstalk between the mTOR and MAPK/ERK pathways can be problematic when both pathways are inhibited separately and may lead to a poor drug response (16). Consequently, as HSP90 inhibition suppresses the signaling of proteins within both pathways simultaneously (15), this may be a more effective approach than e.g. the mTOR inhibitor, everolimus, that was approved for the treatment of NETs in 2016 following the RADIANT trials (17-19).

Several HSP90 inhibitors have been assessed preclinically and in clinical trials (20). However, treatment success has often been limited due to poor solubility and hepatotoxicity. This has led to the development of second-generation HSP90 inhibitors (21). One such promising agent is onalespib, a second-generation HSP90 inhibitor currently being tested in clinical trials. It is administered both as a monotherapy and in combination with other chemotherapeutic drugs, in various types of solid tumors, including NETs (22). In a recent preclinical study, onalespib displayed potent radiosensitizing properties when used in combination with external beam irradiation (23). Although the mechanisms behind the radiosensitizing properties of onalespib are not yet fully understood, there are several indications for the involvement of DDR (23).

Consequently, the dual role of onalespib, as both a NET antitumorigenic agent and a radiotherapy potentiator, may render it an optimal candidate for use in combination with ^{177}Lu-DOTATATE in NETs. ^{177}Lu-DOTATATE is already established as a therapeutic option with the local delivery of radiation to tumor lesions. The addition of onalespib could affect proliferation and survival and may act as a radiosensitizer through the regulation of DDR. Therefore, the aim of this study was to investigate whether the HSP90 inhibitor onalespib, can reduce NET growth and act as a radiosensitizer when used in combination with ^{177}Lu-DOTATATE. This was assessed *in vitro*, measuring the therapeutic effects of both treatments as monotherapies and in combination, as well as by investigating the molecular effects of the treatments.

Materials and methods

Cell lines. The human cell line, BON (24), established from a lymph node metastasis of a carcinoid tumor of the pancreas, was kindly provided by Professor Townsend (The University of Texas Medical Branch, Texas University) and grown in DMEM/Ham's F12 1:1 (Biochrome) supplemented with 10% fetal bovine serum (Sigma-Aldrich), L-glutamine and antibiotics (100 IU penicillin and 100 μg/ml streptomycin) from (Biochrome). The NCI-H727 (CRL-5815) cells (25), a well differentiated neuroendocrine cell line derived from a human lung carcinoid, and the NCI-H460 (HTB-177) cells (25,26), a large cell lung carcinoma human cell line with neuroendocrine features, were purchased from ATCC and grown in RPMI-1640 (Biochrome) with above-mentioned supplements. All cells were grown in an incubator with 37˚C and 5% CO_2 and cultivated according to good cell culture practice.

Drug and radioconjugate preparation. Onalespib (Selleckchem) was stored at -20˚C as a lyophilized powder. Prior to drug treatment, it was dissolved in DMSO to a concentration of 122.1 mM and subsequently diluted in cell media.

For DOTATATE labeling, 1.5 μg DOTATATE (Bachem) dissolved in water was mixed with reaction buffer (25 mM sodium ascorbate/50 mM sodium acetate, pH 5) and 60 MBq ^{177}Lu (ITG GmbH). The reaction vial was incubated at 80˚C for 30 min. The labeling yield was assessed with instant thin layer chromatography (Biodex Medical Systems) and sodium citrate (0.1 M, pH 5.5) as mobile phase, with subsequent quantification in a phosphoimager (BAS-1800II, Fujifilm).

XTT cell viability assay. The cells ($5x10^3$ BON, $12x10^3$ NCI-H727 or $0.7x10^3$ NCI-H460 cells) were seeded in 96-well plates and incubated at 37˚C for 1-2 days. The medium was then replaced and onalespib was added with concentrations ranging from 1-10^4 nM. After 72 h, an XTT assay (301011K, LGC Standards) was performed according to the manufacturer's instructions. Briefly, 80 μl XTT activation reagent and 4 ml XTT reagent were mixed and added to 8 ml cell medium. The old medium was removed and 150 μl were added to each well. The plates were then incubated for 4 h at 37˚C and analyzed using a plate reader (Bio-Rad Laboratories).

Cellular uptake of ^{177}Lu-DOTATATE. The cells ($4x10^4$ BON, $4x10^4$ NCI-H727 or $1.5x10^4$ NCI-H460 cells) were seeded in 24-well plates and incubated at 37˚C for 48 h. ^{177}Lu-DOTATATE was added at a final concentration of 20 nM. Following 24 h of incubation at 37˚C, unbound ^{177}Lu-DOTATATE was removed and the cells were trypsinized. Cell-associated activity was counted in a gamma counter (1480 Wizard 3', Wallace).

Multicellular tumor spheroids. Agarose-coated 96-well plates were prepared as previously described (27). A total of $5x10^3$ BON, $3x10^3$ NCI-H727 or $1.5x10^3$ NCI-H460 cells were then seeded. Following spheroid formation (3-4 days), onalespib (25-100 nM) and/or ^{177}Lu-DOTATATE (1-50 kBq) was added daily for 3 days. Onalespib was added 3 h prior to ^{177}Lu-DOTATATE. The spheroids were photographed every 2-3 days using a Canon EOS 700D (Canon, Inc.) mounted on a Nikon Diaphot-TMD microscope (Nikon) and media was added or exchanged 1-2 times per week. The cross-section area was measured using Fiji and the volume of each spheroid was calculated (28). All spheroids were followed individually and normalized to the size at the start of treatment.

Western blot analysis. The BON cell spheroids were treated with 25 nM onalespib and/or 5 kBq ^{177}Lu-DOTATATE. At 24 h post-treatment, whole cell lysates were prepared with lysis buffer: 1% NP-40 Alternative, 20 mM Tris (pH 8.0), 137 mM NaCl, 10% glycerol, 2 mM EDTA, 1 mM heat activated sodium orthovanadate Na3VO4, (95 C for 10 min) and protease inhibitor cocktail (Sigma-Aldrich) for 30 min on ice. The protein concentration was measured using a Nanophotometer P-Class (Implen). The samples were equalized to a relative protein amount and equal volumes of protein lysates were separated by SDS-PAGE [Tris-Acetate 3-8% gel (ThermoFisher Scientific)] and transferred onto a nitrocellulose membrane (Immobilon-P

Transfer membrane, Millipore) by wet blotting for 24 h at 4˚C followed by blocking of the membrane for 1 h in PBS with 5% BSA. The membrane was divided according to the size of the expected proteins and the slices were incubated with the according rabbit monoclonal anti-EGFR (1:5,000, ab52894, Abcam), mouse monoclonal anti-SSTR5 (1:1,000, ab109495, Abcam), rabbit polyclonal anti-HSP90 (1:20,000, ab13495, Abcam), mouse monoclonal anti-β-actin (1:10,000, A5441, Sigma-Aldrich), mouse monoclonal anti-γ H2A histone family member X (γH2AX; 1:1,000, 05-636, Merck/Millipore), rabbit monoclonal anti-IGF1-R (1:1,000, ab182408, Abcam), polyclonal mTOR (1:2,000, ab2732, Abcam), mouse monoclonal anti-ERK1 + ERK2 (1:2,000, ab54230, Abcam), rabbit monoclonal anti-AKT1/2/3 (1:10,000, ab179463, Abcam), rabbit monoclonal anti-sodium potassium ATPase (1:2,000, ab76020, Abcam), rabbit polyclonal anti-phosphatase and tensin homolog (PTEN; 1:1,000, #9552, Cell Signaling Technologies) rabbit polyclonal H2AX (1:10,000, ab11175, Abcam) antibodies at 4˚C overnight. The membrane was rinsed in PBS-Tween (0.1%) and incubated with species-specific horseradish peroxidase-labeled secondary antibodies (anti-mouse 1:3,000, #65-6520, ThermoFisher Scientific; anti-rabbit 1:5,000, #65-6120, ThermoFisher Scientific) for 1 h at room temperature. Electro-chemiluminescent solution (Immobilon, Millipore) was applied and immunoreactive bands were visualized with a CCD camera (SuperCCD HR, Fujifilm). Image analysis and quantification of the bands was evaluated using ImageJ 1.48v software (NIH). The total protein expression levels were adjusted to the corresponding loading control (β-actin or sodium potassium ATPase) according to the following formula: Total protein expression=band intensity protein/band intensity loading control. The total protein expression level was then normalized to the intensity level of the adjusted untreated control sample (untreated control level=1). To further evaluate the expression of yH2AX compared to unphosphorylated protein (H2AX) the following formula was used: Total yH2AX expression (z)=the band intensity yH2AX/band intensity of H2AX. The error analysis of yH2AX (Dz) was performed with the equation Dz/z=Sum[(Da/a)2+(Db/b)2+(Dc/c)2], where each value (a, b, c) has an associated standard deviation (Da, Db or Dc, respectively).

Flow cytometry. BON spheroids were seeded and treated as described above with 25 nM onalespib and/or 5 kBq ^{177}Lu-DOTATATE. At 24 h after final treatment, the spheroids were trypsinized and resuspended in PBS. The cells were then incubated with 2 μM CellEvent™ Caspase 3/7 Green Detection Reagent (Thermo Fisher Scientific) for 15 min at room temperature, protected from light. Sytox Red Dead Cell Stain (Thermo Fisher Scientific) was added at a final concentration of 5 nM and the cells were incubated at room temperature for an additional 15 min. The cells were then filtered through a CellTrics 50 μm filter (Sysmex) and analyzed using a flow cytometer (CyFlow Space, Sysmex). Data analysis was performed with the FCGUI Toolbox for Matlab 2016b (Mathworks).

Statistical analysis. Data are presented as the means ± standard deviation if not otherwise stated. Statistical analysis was performed using Graphpad Prism 7 software (GraphPad Software), where a P-value ≤0.05 was considered to indicate a statistically significant difference. In viability assays, IC50 calculations (50% of maximal inhibition) were made in Graphpad by fitting the data to a dose-response curve (standard slope) according to the following equation:

$$y = a + \frac{100 - a}{1 + 10^{x - \log(IC50)}}$$

where y is viability in %, a is minimum response and x is $\log_{10}$(concentration) of onalespib. For spheroid assays, one-way ANOVA with Dunnett's (dose-response of monotherapies) or Tukey's (combination assays) multiple comparison. Synergy calculations was performed according to the Chou-Talalay (29) method with Compusyn (Combosyn). Western blot data was analyzed using one-way ANOVA and Tukey's multiple comparison.

Results

Characterization of cell lines

Onalespib reduced viability in monolayer NET cells. The effects of onalespib on monolayer cell cultures were assessed by XTT cell viability assays (Fig. 1A). All cell lines were found to be sensitive to onalespib treatment and the calculated IC50 values were 27 nM (95% CI 19-39 nM) for the BON, 102 nM (95% CI 78-132 nM) for the NCI-H727 and 51 nM (95% CI 38-69 nM) for the NCI-H460 cells.

^{177}Lu-DOTATATE uptake in NET cell lines. The uptake of ^{177}Lu-DOTATATE was assessed by measuring the cell-associated radioactivity 24 h following the addition of the compound. The uptake of ^{177}Lu-DOTATATE was observed in the BON and NCI-H727 cells at similar levels, while the NCI-H460 cells exhibited no detectable uptake (Fig. 1B). From these results, the BON and NCI-H727 cells were defined in this study as SSTR-positive and the NCI-H460 cells were defined as SSTR-negative. The ^{177}Lu-DOTATATE uptake in the SSTR-positive cell lines was not affected by treatment with onalespib (Fig. S1).

Multicellular tumor spheroids. Multicellular tumor spheroids mimic *in vivo*-like conditions, with nutrient and oxygen gradients within the spheroid similar to those in tumors. Moreover, it is a relevant model for PRRT due to the three-dimensional distribution of the emitted radiation. In the current study, spheroids were treated with daily concentrations of onalespib, ranging from 25-100 nM and 1-50 kBq ^{177}Lu-DOTATATE on 3 consecutive days. Spheroid size was measured at 14 (NCI-H460) or 20 (BON, NCI-H727) days following the start of treatment.

Growth inhibitory effect of onalespib and ^{177}Lu-DOTATATE as monotherapies. Onalespib exerted growth inhibitory effects on all cell lines (Fig. 2, A, D and G). With a concentration of 50 nM, the spheroid size compared to the untreated cells was 46±10, 26±3 and 40±5% for the BON (Fig. 2A), NCI-H727 (Fig. 2D) and NCI-H460 (Fig. 2G) cells, respectively. DMSO had no marked effect on spheroid growth (Fig. S2). It was found that ^{177}Lu-DOTATATE significantly inhibited the growth of the BON (Fig. 2B) and NCI-H727 (Fig. 2E) cell-derived spheroids. However, ^{177}Lu-DOTATATE had no effect on the spheroid growth of SSTR-negative NCI-H460 cells (Fig. 2H). These results were in accordance

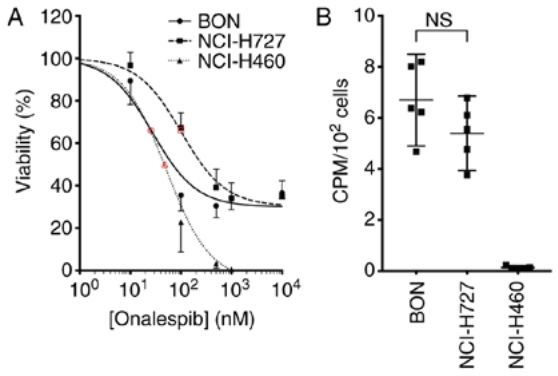

Figure 1. Characterization of cell lines. (A) XTT viability assay of monolayer cultures. Graph displays viability (%) on the y axis (mean and 95% CI, n=6) and concentration (nM) on the x axis. Red open symbols indicate 50% of maximal inhibition. Corresponding calculated IC50 values were 27 nM for the BON (solid line), 102 nM for the NCI-H727 (dashed line) and 51 nM for the NCI-H460 (dotted line) cells. (B) Uptake of ^{177}Lu-DOTATATE in monolayer cultures. Graph displays CPM/10^2 cells (mean and 95% CI, n=6); n.s, not significant.

with the SSTR status. Following treatment with 50 kBq ^{177}Lu-DOTATATE, the spheroid size compared to the untreated cells was 25±3, 41±3 and 91±9% in the BON, NCI-H727 and NCI-H460 cells, respectively. Unlabeled DOTATATE did not have a marked effect on spheroid growth (Fig. S2).

Specific and synergistic effects in the spheroids treated with the combined treatment. The combined treatment of the spheroids with onalespib and ^{177}Lu-DOTATATE (Fig. 3) resulted in additional growth inhibitory effects compared to monotherapies in the SSTR-positive cell lines, BON and NCI-H727. In the NCI-H460 cells, no treatment combinations led to any significantly differences compared to onalespib monotherapy. Additional combinations were tested, with significant differences already observed at day 14 for the BON and NCI-H727 cell-derived spheroids (Fig. S3).

Synergy calculations were performed according to the Chou-Talalay method for the BON and NCI-H727 cells, where a combination index (CI) of <1 indicated synergy. Table I displays results of the synergy calculations for various combinations on days 14 and 20. All tested combinations were synergistic in the BON cell-derived spheroids, while in the NCI-H727 cells, synergy was present following treatment with 40 nM onalespib.

Combination treatment downregulates EGFR expression and increases apoptosis. To further determine the molecular effects of onalespib and ^{177}Lu-DOTATATE, western blot analysis and flow cytometry were performed on the BON cell-derived spheroids (Fig. 4). EGFR, a client protein of HSP90, mediates the signaling of cell proliferation and survival e.g., by initiating the mTOR and MAPK/ERK signaling pathways (20). In this study, onalespib treatment resulted in the downregulation of EGFR, while ^{177}Lu-DOTATATE had no effect (Fig. 4A and B). The spheroids treated with the combination treatments exhibited the lowest EGFR expression. Compared to the untreated control, EGFR expression was 78±7, 109±12 and 64±5% in the spheroids treated with onalespib, ^{177}Lu-DOTATATE and their combination, respectively. No significant differences in HSP90 expression were detected (Fig. 4A and C).

γH2AX expression can be used to indicate the level of DNA double-strand breaks. The spheroids treated with onalespib or the combination treatment both exhibited significantly higher levels of γH2AX (Fig. 4A and D) compared to the untreated spheroids, whereas ^{177}Lu-DOTATATE alone did not markedly affect γH2AX expression compared the untreated spheroids. Combined treatment did not lead to significant differences in γH2AX expression compared to treatment with onalespib alone. γH2AX expression in the spheroids normalized to the untreated cell was 181±64, 104±39 and 216±167% for the cells treated with onalespib, ^{177}Lu-DOTATATE and the combination treatment, respectively.

Caspase 3 and 7 are commonly used as markers of apoptosis. In this study, flow cytometry was used to quantify the amount of caspase 3/7 in the cells. There was a 2-fold increase in caspase 3/7 activity in the combination treated spheroids, while treatment with onalespib or ^{177}Lu-DOTATATE alone had no effect on caspase activity (Figs. 4E and S4).

To further investigate the involvement of the mTOR and MAPK/ERK signaling pathways, the levels of IGF1-R, as well as a number of downstream targets were assessed by western blot analysis (Fig. 4A and F-J). In general, the levels of the assessed proteins followed the same pattern as that of EGFR, with decreased levels in the onalespib and combination-treated samples. For IGF1-R and mTOR, these changes were however, not statistically significant. ERK expression was downregulated following treatment with onalespib and combination treatment, with the lowest levels observed in the spheroids treated with the combination treatment (57±23% of the untreated control). AKT and PTEN expression levels were downregulated by onalespib (47±14 and 46±5% of the untreated control, respectively); however, a significant effect was also observed following ^{177}Lu-DOTATATE monotherapy (77±14 and 64±18%, respectively). Combination treatment resulted in AKT and PTEN levels similar to those from onalespib treatment.

Discussion

PRRT with ^{177}Lu-DOTATATE has revolutionized the treatment of SSTR-positive NETs (2). However, despite a marked increase in disease-free survival, a complete response is rare. The combined use of PRRT with radiosensitizers may be a promising strategy with which to potentiate the treatment efficacy, enabling a systemic dual targeting treatment. HSP90 was recently proposed as a target for NET therapy, and the HSP90 inhibitor onalespib has previously demonstrated radiosensitizing properties in combination with external radiotherapy (23).

In the present study, we examined efficacy of the HSP90 inhibitor, onalespib, on a panel of NET cell lines in monolayer cultures (Fig. 1), as well as in multicellular tumor spheroids (Fig. 2), demonstrating antitumorigenic activity in all the cell lines examined. These findings are in line with those of previous studies validating the high potential of HSP90 inhibitors for NETs (12,14,15).

The effect of ^{177}Lu-DOTATATE on spheroid growth was then assessed on the NET cell lines, BON (pancreatic carcinoid), NCI-H727 (bronchial carcinoid) and NCI-H460

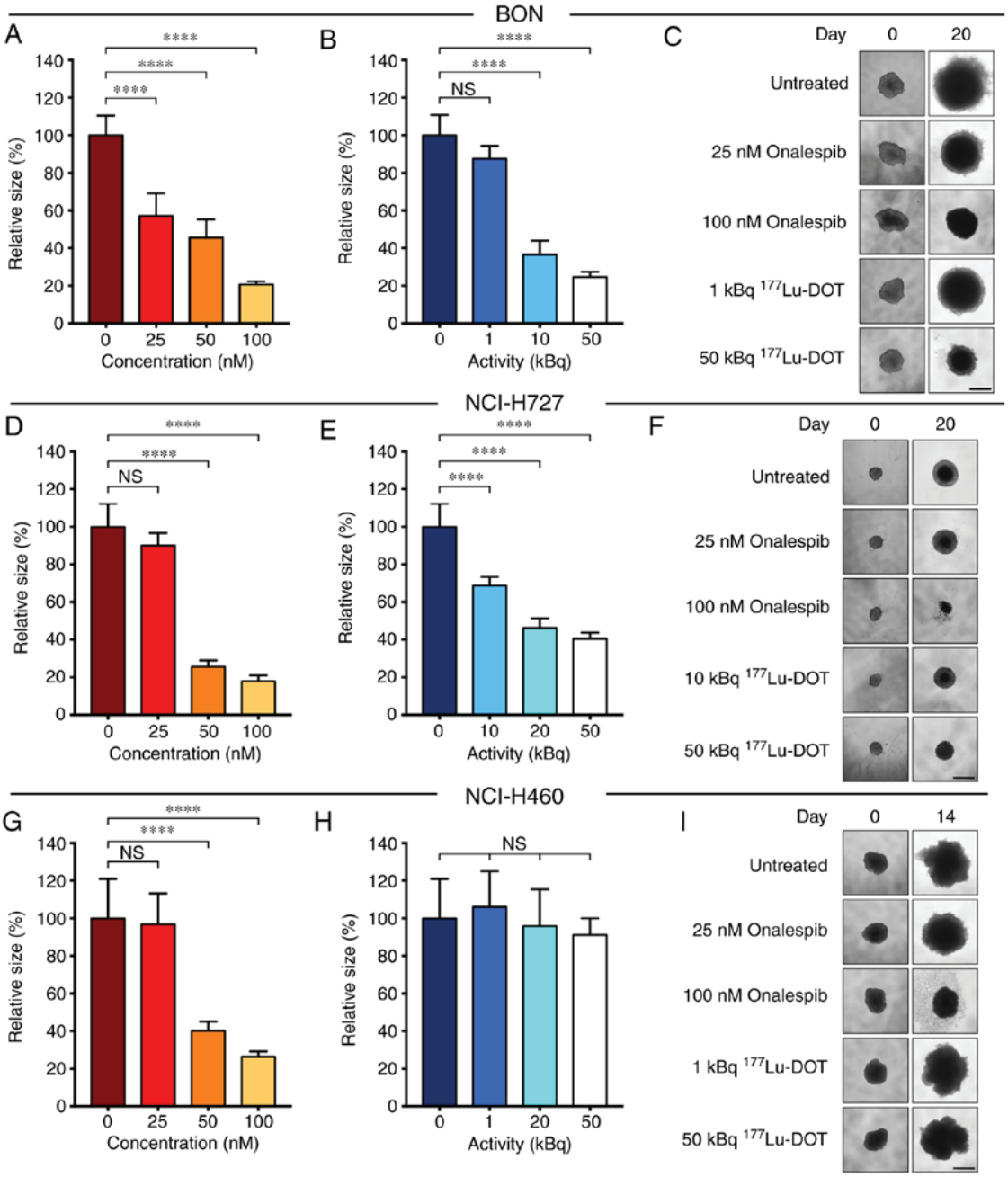

Figure 2. Monotherapy with onalespib or ^{177}Lu-DOTATATE in spheroids. Growth of spheroids treated with (A, D and G) onalespib or (B, E and H) ^{177}Lu-DOTATATE at day 14 (NCI-H460 cells) or day 20 (BON and NCI-H727 cells) with representative spheroid images (C, F and I) for the (A-C) BON, (D-F) NCI-H727 and (G-I) NCI-H460 cell-derived spheroids. Spheroids were treated with a daily concentration indicated in the graphs. Graphs display size normalized to the untreated cells (means ± standard deviation, n≥4); scale bar, 500 μm. ^{177}Lu-DOT, ^{177}Lu-DOTATATE. ****P≤0.0001; n.s., not significant.

(large cell lung carcinoma). As expected, treatment resulted in the growth inhibition of SSTR-positive cell lines, while the SSTR-negative NCI-H460 cell line was unaffected. As the NCI-H460 cell line is a large cell carcinoma with different biological and pathological features from the carcinoids, it is not surprising that this cell line differed from the other two in SSTR expression (25). Moreover, unlabeled DOTATATE in equivalent concentrations had no effect on spheroid growth (Fig. S2). These results confirm the specificity of ^{177}Lu-DOTATATE treatment.

Furthermore, when onalespib and ^{177}Lu-DOTATATE (Fig. 3) were used in combination, the growth inhibitory effects on the BON and NCI-H727 cell-derived spheroids were even more pronounced than the corresponding monotherapies. Following combined treatment, the BON cells exhibited synergistic effects for all tested concentrations and time points. Synergy was also found in the NCI-H727 cells and was most pronounced at 20 days following treatment. Low concentrations of onalespib led to an additive effect on NCI-H727 cell-derived spheroids. As the Chou-Talalay method requires both drugs to demonstrate a significant effect and ^{177}Lu-DOTATATE had no effect on NCI-H460 cells, no synergy calculations were performed for this cell line. However, as none of the combination treatments led to significant differences compared to onalespib monotherapy, ^{177}Lu-DOTATATE was not able to enhance the effects of onalespib or vice versa in the NCI-H460

Table I. Synergistic analysis of BON and NCI-H727 cells.

	Onalespib (nM)	^{177}Lu-DOT (kBq)	CI day 14	CI day 20
BON	10	10	0.40[a]	n.a.
	25	1	n.a.	0.50
	25	5	0.46	0.39[a]
	25	10	0.45[a]	0.65
	25	20	0.62[a]	n.a.
NCI-H727	25	50	1.45	n.a.
	40	10	1.02	0.67[a]
	40	20	0.65[a]	0.62[a]
	40	50	0.69[a]	n.a.

Combination Index (CI) was calculated with the Chou-Talalay method (29). CI<1 indicates synergy, CI=1 indicates additivity and CI>1 indicates antagonism. [a]Combination therapy led to significant differences from the corresponding monotherapies. n.a., not analyzed.

cells. Consequently, it was concluded that the combination of onalespib and ^{177}Lu-DOTATATE is synergistic and specific for SSTR-positive NETs.

After the growth inhibitory effects of monotherapy and the combination treatments had been verified, the responses at the molecular level were investigated. One way to validate the molecular effects of onalespib is by assessing EGFR expression. EGFR, an HSP90 client protein, is an activator of the mTOR and MAPK/ERK pathways, which are highly relevant in NET tumorigenesis (20,30,31). Blocking these pathways by the downregulation of growth factor receptors, such as EGFR can enhance the therapeutic response. The results from western blot analysis of EGFR expression (Fig. 4A and B) demonstrated the downregulation in the onalespib-treated BON spheroids, consistent with the findings of previous studies (23,32). ^{177}Lu-DOTATATE treatment did not affect EGFR expression. Notably, the lowest level of EGFR expression was observed in the combination treatment group. The reason for this is not clear. One potential explanation could be radiotherapy-induced HSP90 cleavage. It is known that radiotherapy increases the level of reactive oxygen species (ROS). Several studies have investigated the association between ROS and HSP90, finding that ROS can cleave HSP90 at the N-terminal, leading to the loss of function and additional client protein degradation (33,34). However, this could not be confirmed in HSP90 expression analyses (Fig. 4A and C), where no differences in HSP90 expression were observed between the treatment groups. Nonetheless, the clear decrease in EGFR expression in the onalespib-treated samples verify the growth inhibitory effects of the drug, and point to an even more effective outcome when used in combination with ^{177}Lu-DOTATATE. This was further supported by the results from western blot analysis of additional proteins involved in the mTOR and MAPK/ERK signaling pathways (Fig. 4A and F-J).

HSP90 plays an important role in DDR (11). In this study, we investigated DDR by investigating the DNA double-strand break marker, γH2AX, 24 h following treatment (Fig. 4A and D). The nuclear expression of γH2AX is a sensitive marker for DNA double-strand breaks, where γH2AX accumulates in foci within seconds after the occurrence of the DNA double-strand breaks, and the level usually peaks within 1 h, followed by decreasing levels proportional to the repair rate. Moreover, pan-nuclear γH2AX staining represents apoptotic signaling, triggered by ATM and DNA-PKcs activation (35). Consequently, as western blot analysis of total γH2AX cannot distinguish between the nuclear and pan-nuclear expression of the protein, γH2AX expression indicates either an insufficient DNA damage repair machinery or induction of apoptosis in this assay. In this study, at 24 h following treatment with ^{177}Lu-DOTATATE, the BON cells were able to repair the induced DNA damage. However, a significant increase in γH2AX expression was observed in the spheroids treated with onalespib and the combination treatment. This suggests that the enhanced growth inhibition in the spheroids treated with onalespib and the combination treatment is in part due to an increased number of double-strand breaks and apoptosis.

To further investigate the involvement of apoptosis, flow cytometry was used to measure caspase 3 and 7 activity at 24 h after final treatment. While no significant increase in caspase 3/7 activity was observed in the onalespib- or ^{177}Lu-DOTATATE-treated spheroids, combination treatment led to a 2-fold increase in caspase activity at this time point. The somewhat different staining profiles of γH2AX, and caspase 3 and 7 indicate different kinetic profiles and/or mechanisms of the investigated events. However, the results suggest that the enhanced growth inhibition in the spheroids treated with the combination treatment is in part due to increased apoptosis.

In conclusion, the present study demonstrates that HSP90 inhibition with onalespib is a feasible treatment option for NETs. Moreover, the combination of onalespib and ^{177}Lu-DOTATATE is particularly promising due to SSTR-specific synergistic effects. The potent synergistic effects observed in the present study are most likely due to several contributing factors, involving the suppression of EGFR signaling and the induction of apoptosis. The combination of onalespib and ^{177}Lu-DOTATATE may improve the therapeutic response for patients with inoperable and metastatic NETs, leading to increased cure rates. Further *in vivo* studies investigating this strategy are required to confirm these promising findings.

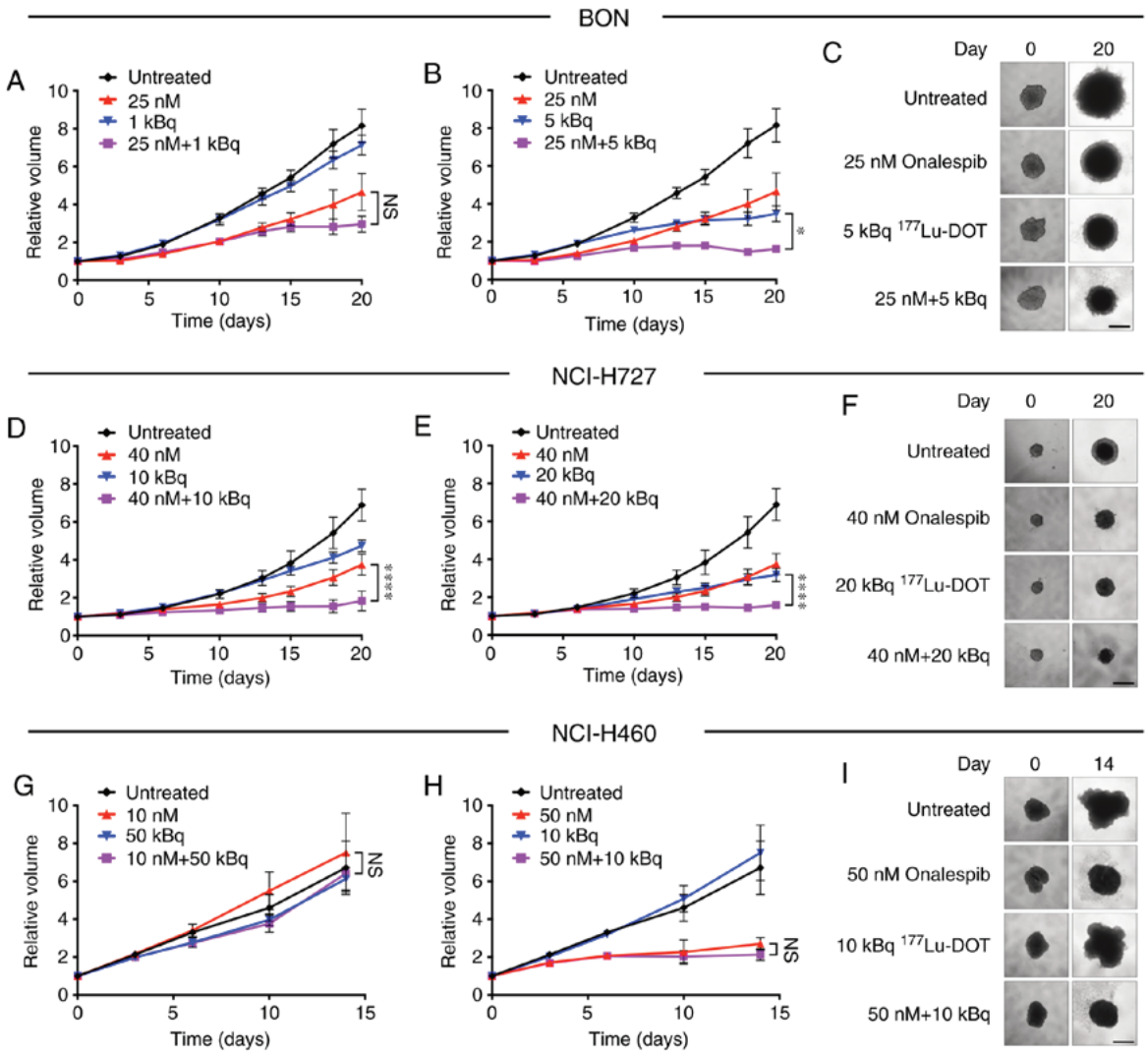

Figure 3. Combination therapy with onalespib and ^{177}Lu-DOTATATE in spheroids. Treatments with onalespib (upward-facing triangles), ^{177}Lu-DOTATATE (downward-facing triangles) and the combination of the two (squares) compared to the untreated (rhombus shapes) cells with representative spheroid images at the first and final time point for the (A-C) BON, (D-F) NCI-H727 and (G-I) NCI-H460 cells. Spheroids were treated with a daily concentration indicated in the graphs. Graphs display volume on the y axis and time on the x axis (means ± standard deviation, n≥4). For combinations that led to significant differences from the monotherapies, the comparison with lowest significance level is displayed. *P≤0.05 and ****P≤0.0001; n.s., not significant. Scale bar, 500 μm.

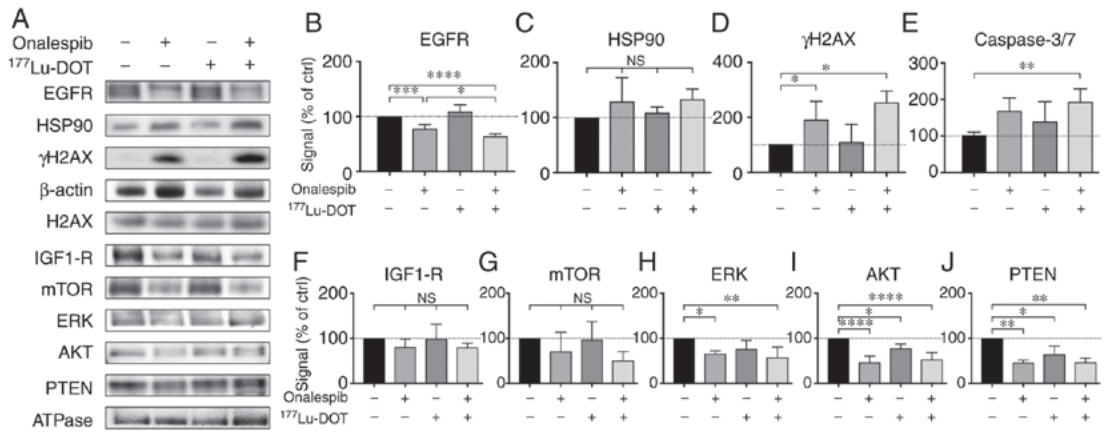

Figure 4. Western blot analysis and flow cytometry of the treated spheroids. (A) Western blot analysis of EGFR, HSP90, IGF1-R, mTOR, ERK, AKT, PTEN and γH2AX 24 h after final treatment. β-actin and Na/K-ATPase were used as loading controls. Representative blots are shown. (B-D and F-J) Western blot analysis quantification of EGFR, HSP90, IGF1-R, mTOR, ERK, AKT, PTEN and γH2AX. Graphs display signal normalized to loading control and to untreated control samples (means ± standard deviation, γH2AX expression was normalized to unphosphorylated protein expression (H2AX; n=3-6). (E) Flow cytometric assessment of caspase 3 and 7 activity in the treated spheroids. *P≤0.05, **P≤0.01, ***P≤0.001 and ****P≤0.0001; n.s, not significant. EGFR, epidermal growth factor receptor; HSP90, heat shock protein 90; IGF1-R, insulin-like growth factor 1; mTOR, mammalian target of rapamycin; ERK, extracellular-signal-regulated kinase; PTEN, phosphatase and tensin homolog; γH2AX, γ H2A histone family member X.

Acknowledgements

The authors would like to thank Dr Andris Abramenkovs, Uppsala University, for assisting with the image analysis, Mrs. Anna Mäkiniemi and Ms. Martina Nilsson, Uppsala University, for assisting in XTT assays and Ms. Noelle Chung, Uppsala University, for performing Western blots.

Funding

This study was supported by grants from the Swedish Cancer Society (CAN 2018/494, CAN2016/649, CAN 2015/1080 and CAN 2015/385), the Swedish Research Council (2013-30876-104113-30), Torsten and Ragnar Söderbergs Foundation for Oncological Endocrinology, and Lennart Glans Foundation.

Availability of data and materials

All data generated or analyzed during this study are included in this published article.

Authors' contributions

SL contributed to the design of the study and contributed to the major part of the experimental studies (with focus on XTT, spheroid and flow cytometric assays), analyzed and interpreted the data, and drafted and revised the manuscript. DS contributed to the design of the study, contributed to experimental studies (with focus on the western blot analysis experiments), analyzed and interpreted data and revised the manuscript. BS contributed to the design of the study and data interpretation, and revised the manuscript. MN initiated and designed the study, contributed to data analysis and interpretation and revised the manuscript. All authors have read and approved the final manuscript.

Ethics approval and consent to participate

Not applicable.

Patient consent for publication

Not applicable.

Competing interests

The authors declare that they have no competing interests.

References

1. Krenning EP, Kooij PP, Bakker WH, Breeman WA, Postema PT, Kwekkeboom DJ, Oei HY, de Jong M, Visser TJ, Reijs AE, *et al*: Radiotherapy with a radiolabeled somatostatin analogue, [111In-DTPA-D-Phe1]-octreotide. A case history. Ann N Y Acad Sci 733: 496-506, 1994.
2. Strosberg J, El-Haddad G, Wolin E, Hendifar A, Yao J, Chasen B, Mittra E, Kunz PL, Kulke MH, Jacene H, *et al*: Phase 3 trial of ^{177}Lu-dotatate for midgut neuroendocrine tumors. N Engl J Med 376: 125-135, 2017.
3. Kratochwil C, Lopez-Benitez R, Mier W, Haufe S, Isermann B, Kauczor HU, Choyke PL, Haberkorn U and Giesel FL: Hepatic arterial infusion enhances DOTATOC radiopeptide therapy in patients with neuroendocrine liver metastases. Endocr Relat Cancer 18: 595-602, 2011.
4. Virgolini I, Patri P, Novotny C, Traub T, Leimer M, Füger B, Li SR, Angelberger P, Raderer M, Wogritsch S, *et al*: Comparative somatostatin receptor scintigraphy using in-111-DOTA-lanreotide and in-111-DOTA-Tyr3-octreotide versus F-18-FDG-PET for evaluation of somatostatin receptor-mediated radionuclide therapy. Ann Oncol 12 (Suppl 2): S41-S45, 2001.
5. Claringbold PG, Price RA and Turner JH: Phase I-II study of radiopeptide 177Lu-octreotate in combination with capecitabine and temozolomide in advanced low-grade neuroendocrine tumors. Cancer Biother Radiopharm 27: 561-569, 2012.
6. Kratochwil C, Giesel FL, Bruchertseifer F, Mier W, Apostolidis C, Boll R, Murphy K, Haberkorn U and Morgenstern A: ^{213}Bi-DOTATOC receptor-targeted alpha-radionuclide therapy induces remission in neuroendocrine tumours refractory to beta radiation: A first-in-human experience. Eur J Nucl Med Mol Imaging 41: 2106-2119, 2014.
7. Chan HS, Konijnenberg MW, Daniels T, Nysus M, Makvandi M, de Blois E, Breeman WA, Atcher RW, de Jong M and Norenberg JP: Improved safety and efficacy of ^{213}Bi-DOTATATE-targeted alpha therapy of somatostatin receptor-expressing neuroendocrine tumors in mice pre-treated with L-lysine. EJNMMI Res 6: 83, 2016.
8. Miederer M, Henriksen G, Alke A, Mossbrugger I, Quintanilla-Martinez L, Senekowitsch-Schmidtke R and Essler M: Preclinical evaluation of the alpha-particle generator nuclide 225Ac for somatostatin receptor radiotherapy of neuroendocrine tumors. Clin Cancer Res 14: 3555-3561, 2008.
9. Maier P, Hartmann L, Wenz F and Herskind C: Cellular pathways in response to ionizing radiation and their targetability for tumor radiosensitization. Int J Mol Sci 17: pii: E102, 2016.
10. Den RB and Lu B: Heat shock protein 90 inhibition: Rationale and clinical potential. Ther Adv Med Oncol 4: 211-218, 2012.
11. Pennisi R, Ascenzi P and di Masi A: Correction: Pennisi, R., *et al*. Hsp90: A new player in DNA repair? Biomolecules 2015, 5, 2589-2618. Biomolecules 6: pii: E40, 2016.
12. Gilbert JA, Adhikari LJ, Lloyd RV, Halfdanarson TR, Muders MH and Ames MM: Molecular markers for novel therapeutic strategies in pancreatic endocrine tumors. Pancreas 42: 411-421, 2013.
13. Gilbert JA, Adhikari LJ, Lloyd RV, Rubin J, Haluska P, Carboni JM, Gottardis MM and Ames MM: Molecular markers for novel therapies in neuroendocrine (carcinoid) tumors. Endocr Relat Cancer 17: 623-636, 2010.
14. Gloesenkamp C, Nitzsche B, Lim AR, Normant E, Vosburgh E, Schrader M, Ocker M, Scherübl H and Höpfner M: Heat shock protein 90 is a promising target for effective growth inhibition of gastrointestinal neuroendocrine tumors. Int J Oncol 40: 1659-1667, 2012.
15. Zitzmann K, Ailer G, Vlotides G, Spoettl G, Maurer J, Göke B, Beuschlein F and Auernhammer CJ: Potent antitumor activity of the novel HSP90 inhibitors AUY922 and HSP990 in neuroendocrine carcinoid cells. Int J Oncol 43: 1824-1832, 2013.
16. Mendoza MC, Er EE and Blenis J: The Ras-ERK and PI3K-mTOR pathways: Cross-talk and compensation. Trends Biochem Sci 36: 320-328, 2011.
17. Yao JC, Shah MH, Ito T, Bohas CL, Wolin EM, Van Cutsem E, Hobday TJ, Okusaka T, Capdevila J, de Vries EG, *et al*: Everolimus for advanced pancreatic neuroendocrine tumors. N Engl J Med 364: 514-523, 2011.
18. Yao JC, Fazio N, Singh S, Buzzoni R, Carnaghi C, Wolin E, Tomasek J, Raderer M, Lahner H, Voi M, *et al*: Everolimus for the treatment of advanced, non-functional neuroendocrine tumours of the lung or gastrointestinal tract (RADIANT-4): A randomised, placebo-controlled, phase 3 study. Lancet 387: 968-977, 2016.
19. Fazio N, Granberg D, Grossman A, Saletan S, Klimovsky J, Panneerselvam A and Wolin EM: Everolimus plus octreotide long-acting repeatable in patients with advanced lung neuroendocrine tumors: Analysis of the phase 3, randomized, placebo-controlled RADIANT-2 study. Chest 143: 955-962, 2013.
20. Hong DS, Banerji U, Tavana B, George GC, Aaron J and Kurzrock R: Targeting the molecular chaperone heat shock protein 90 (HSP90): Lessons learned and future directions. Cancer Treat Rev 39: 375-387, 2013.
21. Shapiro GI, Kwak E, Dezube BJ, Yule M, Ayrton J, Lyons J and Mahadevan D: First-in-human phase I dose escalation study of a second-generation non-ansamycin HSP90 inhibitor, AT13387, in patients with advanced solid tumors. Clin Cancer Res 21: 87-97, 2015.

22. National Library of Medicine. National Institutes of Health: Onalespib, Dabrafenib, and trametinib in treating patients with BRAF-mutant melanoma or solid tumors that are metastatic or cannot Be removed by surgery, 2019.
23. Spiegelberg D, Dascalu A, Mortensen AC, Abramenkovs A, Kuku G, Nestor M and Stenerlöw B: The novel HSP90 inhibitor AT13387 potentiates radiation effects in squamous cell carcinoma and adenocarcinoma cells. Oncotarget 6: 35652-35666, 2015.
24. Townsend CM Jr, Ishizuka J and Thompson JC: Studies of growth regulation in a neuroendocrine cell line. Acta Oncol 32: 125-130, 1993.
25. Gazdar AF, Helman LJ, Israel MA, Russell EK, Linnoila RI, Mulshine JL, Schuller HM and Park JG: Expression of neuroendocrine cell markers L-dopa decarboxylase, chromogranin A, and dense core granules in human tumors of endocrine and nonendocrine origin. Cancer Res 48: 4078-4082, 1988.
26. Banks-Schlegel SP, Gazdar AF and Harris CC: Intermediate filament and cross-linked envelope expression in human lung tumor cell lines. Cancer Res 45: 1187-1197, 1985.
27. Friedrich J, Seidel C, Ebner R and Kunz-Schughart LA: Spheroid-based drug screen: Considerations and practical approach. Nat Protoc 4: 309-324, 2009.
28. Schindelin J, Arganda-Carreras I, Frise E, Kaynig V, Longair M, Pietzsch T, Preibisch S, Rueden C, Saalfeld S, Schmid B, *et al*: Fiji: An open-source platform for biological-image analysis. Nat Methods 9: 676-682, 2012.
29. Chou TC and Talalay P: Quantitative analysis of dose-effect relationships: The combined effects of multiple drugs or enzyme inhibitors. Adv Enzyme Regul 22: 27-55, 1984.
30. Zitzmann K, Ruden J, Brand S, Göke B, Lichtl J, Spöttl G and Auernhammer CJ: Compensatory activation of Akt in response to mTOR and Raf inhibitors-a rationale for dual-targeted therapy approaches in neuroendocrine tumor disease. Cancer Lett 295: 100-109, 2010.
31. Briest F and Grabowski P: PI3K-AKT-mTOR-signaling and beyond: The complex network in gastroenteropancreatic neuroendocrine neoplasms. Theranostics 4: 336-365, 2014.
32. Spiegelberg D, Mortensen AC, Selvaraju RK, Eriksson O, Stenerlöw B and Nestor M: Molecular imaging of EGFR and CD44v6 for prediction and response monitoring of HSP90 inhibition in an in vivo squamous cell carcinoma model. Eur J Nucl Med Mol Imaging 43: 974-982, 2016.
33. Beck R, Verrax J, Gonze T, Zappone M, Pedrosa RC, Taper H, Feron O and Calderon PB: Hsp90 cleavage by an oxidative stress leads to its client proteins degradation and cancer cell death. Biochem Pharmacol 77: 375-383, 2009.
34. Beck R, Dejeans N, Glorieux C, Creton M, Delaive E, Dieu M, Raes M, Levêque P, Gallez B, Depuydt M, *et al*: Hsp90 is cleaved by reactive oxygen species at a highly conserved N-terminal amino acid motif. PLoS One 7: e40795, 2012.
35. Ding D, Zhang Y, Wang J, Zhang X, Gao Y, Yin L, Li Q, Li J and Chen H: Induction and inhibition of the pan-nuclear gamma-H2AX response in resting human peripheral blood lymphocytes after X-ray irradiation. Cell Death Discov 2: 16011, 2016.